CNI-1493 inhibits Aβ production, plaque formation, and cognitive deterioration in an animal model of Alzheimer's disease

Michael Bacher,[1] Richard Dodel,[1] Bayan Aljabari[2], Kathy Keyvani,[4] Philippe Marambaud,[3] Rakez Kayed,[5] Charles Glabe,[5] Nicole Goertz,[6] Anne Hoppmann,[6] Norbert Sachser,[6] Jens Klotsche,[7] Susanne Schnell,[8] Lars Lewejohann,[6] and Yousef Al-Abed[2]

[1]Department of Neurology, Philipps-University Marburg, 35039 Marburg, Germany
[2]Laboratory of Medicinal Chemistry, [3]Litwin-Zucker Research Center for the Study of Alzheimer's Disease and Memory Disorders, The Feinstein Institute for Medical Research, Manhasset, NY 11030
[4]Institute of Neuropathology, University Hospital Muenster, 48149 Muenster, Germany
[5]Department of Molecular Biology and Biochemistry, University of California, Irvine, Irvine, CA 92697
[6]Department of Behavioural Biology, University of Muenster, 48149 Muenster, Germany
[7]Institute of Clinical Psychology and Psychotherapy, Technical University Dresden, 01187 Dresden, Germany
[8]Department of Neurology, University of Bonn, 53105 Bonn, Germany

Alzheimer's disease (AD) is characterized by neuronal atrophy caused by soluble amyloid β protein (Aβ) peptide "oligomers" and a microglial-mediated inflammatory response elicited by extensive amyloid deposition in the brain. We show that CNI-1493, a tetravalent guanylhydrazone with established antiinflammatory properties, interferes with Aβ assembly and protects neuronal cells from the toxic effect of soluble Aβ oligomers. Administration of CNI-1493 to TgCRND8 mice overexpressing human amyloid precursor protein (APP) for a treatment period of 8 wk significantly reduced Aβ deposition. CNI-1493 treatment resulted in 70% reduction of amyloid plaque area in the cortex and 87% reduction in the hippocampus of these animals. Administration of CNI-1493 significantly improved memory performance in a cognition task compared with vehicle-treated mice. In vitro analysis of CNI-1493 on APP processing in an APP-overexpressing cell line revealed a significant dose-dependent decrease of total Aβ accumulation. This study indicates that the antiinflammatory agent CNI-1493 can ameliorate the pathophysiology and cognitive defects in a murine model of AD.

CORRESPONDENCE
Yousef Al-Abed:
yalabed@nshs.edu

Several studies have investigated the effects of amyloid β protein (Aβ) in the pathogenesis of Alzheimer's disease (AD). Aβ accumulates as amyloid in senile plaques, in the walls of cerebral blood vessels, and in more diffuse immunoreactive deposits in the brains of patients with AD. This accumulation has been implicated in a pathological cascade that ultimately results in neuronal dysfunction and cell death (1, 2). Multiple Aβ species with varying N and C termini are generated from the amyloid β protein precursor (APP) through sequential proteolytic cleavages by the β- and γ-secretases (3). The 40-aa form (Aβ40) is the most abundantly produced Aβ peptide, whereas a slightly longer and less abundant 42-aa form (Aβ42) has been implicated as the more pathogenic species (4). Aβ42 forms aggregate much more readily than Aβ40 and other shorter Aβ peptides, and these aggregates are toxic to a variety of cells in culture. Despite being a minor Aβ species, Aβ42 is deposited earlier and more consistently than Aβ40 in the AD brain.

Recent studies suggest that soluble Aβ peptide "oligomers" (aggregates and/or protofibrils) play an important role in the neuronal atrophy and/or disruption of neural circuits in the cerebral cortex and hippocampus during AD (5, 6). Moreover, the severity of human AD correlates closely with the accumulation of Aβ oligomers rather than other clinical parameters (e.g., senile plaque density) (7–9). Recently, the existence of such Aβ oligomers in human AD brain was demonstrated by use of a specific

M. Bacher and R. Dodel contributed equally to this paper.
The online version of this article contains supplemental material.

antibody that recognizes only oligomeric Aβ, but not monomeric or fibrillar Aβ (10). Collectively, these results suggest that soluble Aβ oligomers present a surface-binding region that is critical for binding to receptors on neuronal synapses and for assembly into amyloid fibrils. In addition to Aβ deposition, neurofibrillary tangle accumulation, and neuronal loss, the end-stage pathology of AD is also notable for the presence of numerous cellular and molecular markers of an inflammatory response that is often associated with the Aβ deposits (11). Accordingly, antiinflammatory drugs have been suggested to be beneficial agents in AD therapy (12).

We use an ELISA-based assay to screen for compounds that might interfere with the binding between Aβ oligomer and the anti-Aβ oligomer antibody. The lead molecule identified with this screen was CNI-1493, a tetravalent guanylhydrazone with well-characterized antiinflammatory activities (13). Systemic administration of CNI-1493 is effective in the treatment of experimental autoimmune encephalomyelitis, cerebral ischemia, and arthritis (14–16). We show that CNI-1493 administration in the APP-expressing TgCRND8 transgenic mice significantly improves memory performance and suppresses the development of amyloid pathology.

RESULTS AND DISCUSSION

CNI-1493 is a surface-directed Aβ oligomer–binding antagonist and is a neuroprotective agent

Because anti-Aβ oligomer antibodies block the toxicity of the "Aβ oligomer" antigen, we hypothesized that compounds that interfere with Aβ oligomer formation and its antibody binding may also interfere with Aβ oligomer receptor binding and/or assembly into amyloid fibril. Accordingly, we screened a library of small molecules and found that CNI-1493 binds to Aβ-oligomer and interferes with its recognition by anti-Aβ oligomer antibodies (Fig. 1 A). To address the question of how CNI-1493 interferes with the Aβ oligomer recognition, we performed electronmicroscopy of Aβ oligomers treated with CNI-1493. As shown in Fig. 1 B, CNI-1493 disrupts the Aβ oligomer. To examine whether the new form of Aβ/CNI-1493 is toxic compared with the Aβ oligomers, we tested the toxicity of Aβ treated with CNI-1493 in the SH-SY5Y neuroblastoma cell line using MTT. As anticipated, the soluble oligomers are toxic (10). Strikingly, soluble oligomers treated with CNI-1493 completely lack Aβ toxicity (Fig. 1 C). Similar neuroprotection was observed in primary neurons: 90 versus 10% survival in those treated with Aβ oligomer in the presence and absence of CNI-1493, respectively (unpublished data). Of note, the neuroprotective effects of CNI-1493 are specific to Aβ oligomer, as evidenced by lack of protection of neuroblastoma cell line when exposed to staurosporine (Fig. S1, available at http://www.jem.org/cgi/content/full/jem.20060467/DC1).

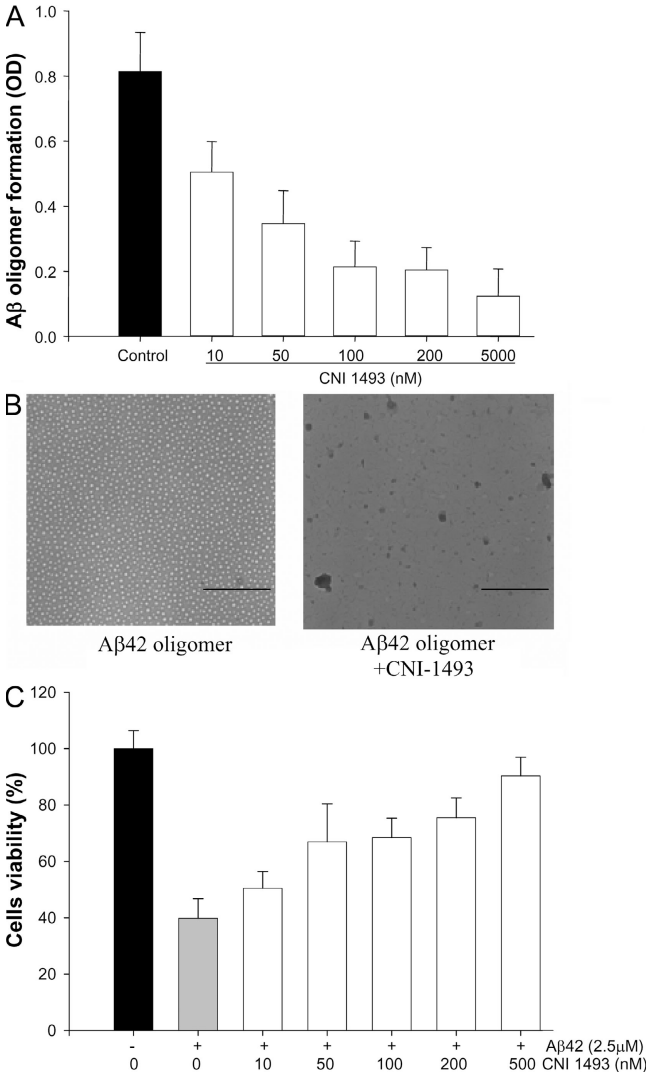

Figure 1. CNI-1493 dose-dependently inhibited Aβ oligomer formation and Aβ oligomer cell toxicity. (A) CNI-1493 inhibits Aβ oligomer formation in vitro as quantified by direct ELISA using anti-Aβ oligomer antibody as described in methods. Control without CNI-1493. (B) CNI-1493 alters the Aβ oligomer fibrillation state. Aβ 42 oligomers were incubated with CNI-1493 at a 10:1 ratio (Aβ oligomer/CNI-1493) for 20 min. The mixture (2 μl) was absorbed onto 200 mesh Nickle carbon, negatively stained with 2% uranyl acetate, and viewed with a microscope. (C) CNI-1493 dose-dependently inhibits cytotoxicity of Aβ oligomers on SH-SY5Y cells as assessed using MTT assay. Control 2.5 μM without CNI-1493, other samples were 2.5 μM Aβ oligomers incubated for 15 min with the indicated concentration of CNI-1493. Error bars represent the SD. Bars, 200 nm.

CNI-1493 prevents the formation of Aβ plaques in APP TgCRND8 transgenic mice

Collectively, the aforementioned experiments indicate that CNI-1493 both interferes with Aβ assembly and protects neurons from their toxic effects. To examine the potential therapeutic effects of CNI-1493 in vivo, we used the transgenic TgCRND8 mouse model, which overexpresses the human APP and manifests many AD features, including cognitive impairment and progressive Aβ plaques formation in their brains at >12 wk of age. CNI-1493 administration was initiated when the mice were 4 mo old. As expected, after 2 mo

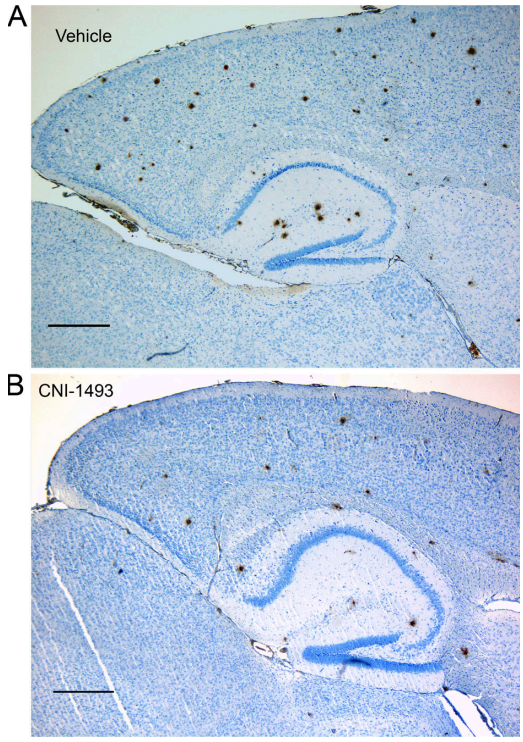

Figure 2. CNI-1493 suppresses Aβ plaque formation in transgenic APP TgCRND8 mice. Sagittal sections from vehicle- or CNI-1493–treated mice were stained for Aβ using the mouse anti-human Aβ monoclonal antibody 6F/3D after 2 mo of treatment. Bar, 500 µm.

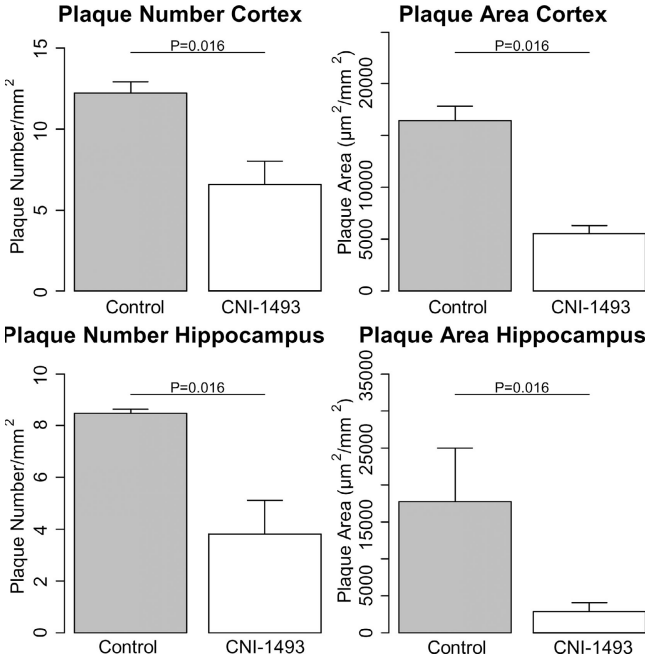

Figure 3. Quantitation of Aβ staining formation reveals a profound reduction of plaque deposition in the CNI-1493–treated TgCRND8 mice relative to that seen in the vehicle-treated mice. CNI-1493 reduced the plaque density in the cortex by 57% (top left; P = 0.016), and in hippocampus by 60% (bottom left; P = 0.016). CNI-1493 reduced plaque area in cortex by 70% (top right; P = 0.016), and in hippocampus by 86% (bottom right; P = 0.016). Digital images from cortex and hippocampus were obtained and analyzed with iSIS analysis Auto Software 3.2. Plaque number was calculated by the number of plaques divided by the area of interest in square millimeter. The plaque area density was computed and expressed as plaque area in square micrometer per area of interest in square millimeters. Statistics, Mann-Whitney U-Tests (two-tailed); control, $n = 5$; CNI-1493, $n = 4$. Error bars represent the SEM.

of treatment (6 mo of age), vehicle-treated mice developed significant Aβ plaque formations (Fig. 2 and Fig. 3). Amyloid deposition was significantly decreased in mice that received CNI-1493 (plaque number divided by the area of interest in square mm was reduced within the cortex by 57% and within the hippocampus by 60% compared with vehicle-treated animals; P = 0.016). This effect by CNI-1493 was even more pronounced when expressed as a reduction of plaque area ratio (area of the plaque in square micrometers divided by the area of interest in square millimeters). We obtained a reduction of 70% within cortex and of 86% within the hippocampus compared with vehicle-treated animals. Significantly, the magnitude of the CNI-1493–mediated decrease in Aβ plaques was not only higher than that reported for the NSAID ibuprofen but was also reached in only 2 mo of treatment, compared with ibuprofen treatment of 4 or 6 mo in Tg2576 APP transgenic mice (17, 18).

CNI-1493 effect on soluble Aβ content in APP TgCRND8 transgenic mice

After demonstrating a potent effect of CNI-1493 on plaque deposition in a relatively short treatment period of 2 mo, we next analyzed the brain cytosol fractions for a possible CNI-1493–dependent regulation of soluble Aβ. As determined by immunoblot analysis, soluble Aβ was significantly reduced in the brains of CNI-1493–treated mice as compared with vehicle-treated mice (Fig. S2).

CNI-1493 deactivates microglia cells in APP TgCRND8 transgenic mice

The mechanisms by which CNI-1493, which is an antiinflammatory agent as well as an amyloid-disrupting assembly agent, affects AD sequelae are likely to be complex and diverse. It has been suggested, however, that one mechanism through which other antiinflammatory agents (e.g., nonsteroidal antiinflammatory drugs [NSAIDs]) exert their therapeutic benefit is through microglia suppression. CNI-1493's role as an antiinflammatory agent has been well established (13), and it has been shown to be effective in animal models of multiple sclerosis, cerebral ischemia, and arthritis (14–16). To examine CNI-1493's effect on microglia in the context of AD, we evaluated microglia activation by analyzing the expression of the microglial surface marker F4/80, which is elevated after activation of these cells (19). We obtained a decrease of F4/80 signal within the brain cytosol of all CNI-1493–treated animals in comparison with control animals (Fig. 4).

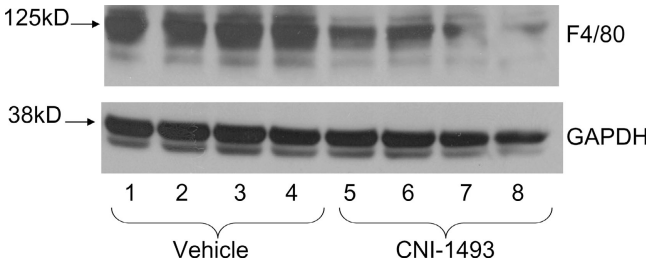

Figure 4. CNI-1493 suppresses microglia activation as assessed by reduced surface marker expression. 60 µg protein were separated by precast NuPAGE Novex 4–12% Bis-Tris gels and transferred onto nitrocellulose membranes using the XCell II blot system. The activation of glial cells was assessed by staining for the macrophage activation with antibodies against the F4/80 antigen. Immunoblot analysis revealed a decline of F4/80 in all CNI-1493 animals. Equal protein loading was assessed by reprobing the membrane with monoclonal antibodies against GAPDH.

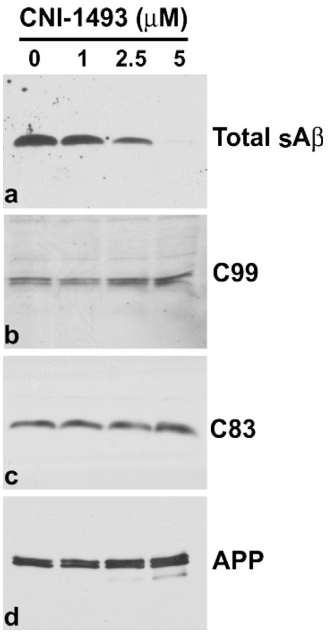

Figure 5. Effect of CNI-1493 on APP processing in N2a cells expressing wild type APP695. Cells were treated for 24 h with the indicated concentrations of CNI-1493. Medium was changed and drug treatment was continued for an additional 4 h to allow Aβ secretion. Total secreted Aβ (total sAβ) was analyzed by immunoblot using 6E10 antibody (a). APP C-terminal fragments, C99 (b), and C83 (c) were analyzed using 6E10 and R1 antibodies, respectively. Full-length APP (d) was tested with antibodies LN27.

The CNI-1493–dependent decrease in total Aβ in N2A cells is unrelated to secretase activities

Several NSAIDs have recently been reported to selectively regulate the processing of APP, and it has been argued that this effect may underlie their beneficial effects in AD (20). NSAID treatment of APP-overexpressing cells was reported to result in a preferential reduction in the production of Aβ42 and a parallel increase in Aβ38, although it had no effect on Aβ40 (20).

In this study, we tested whether CNI-1493 altered total Aβ production in N2a cells overexpressing human APP. CNI-1493 treatment resulted in a dramatic and dose-dependent reduction in the levels of total Aβ secreted into the medium (Fig. 5 A). This result clearly implies that the CNI-1493 effect on APP processing is not restricted to reduction of Aβ42 but also includes the reduction of Aβ40. The observed decrease of total Aβ was not accompanied by reduced levels of APP production (Fig. 6 D). Furthermore, CNI-1493 had no effect on the β- or γ-secretase–mediated cleavage of APP (Fig. 6, B and C), which has recently been proposed for the mode of action of Aβ reduction by ibuprofen (17).

CNI-1493 did not affect spatial memory in TgCRND8 AD mice

Spatial memory was measured using the Barnes maze (21). Both groups, CNI-1493– and placebo-treated mice, showed a reduction in time taken, path length covered, and errors made, indicating spatial memory processes (21). However, analysis of areas under the learning curves as an integrated measure to compare the learning performance did not reveal any significant differences between treatment groups (unpublished data).

CNI-1493 treatment preserves object recognition memory in TgCRND8 AD mice

To measure object recognition memory, mice were observed after presentation with familiar and novel objects. In this paradigm, mice are known to also manifest fear of novel objects, which interferes with the required object exploration (22). Therefore, the experiment was performed on two consecutive days: on day 1, the mice acclimated to the experimental environment; on day 2, we made the experimental observations. Accordingly, the purpose of this study was not to measure changes longitudinally treated from baseline to follow up, but rather to compare the CNI-1493– and placebo-treated groups once the mice were acclimated to the test situation. We measured the recognition index (defined in the Materials and methods) for both the number and time of explorations.

On the first day of analysis, we observed no statistical differences between the CNI-1493– and placebo-treated animals in the recognition indices for either recognition index for number of exploration (0.64 ± 0.07 vs. 0.64 ± 0.09, respectively; $P = 0.99$) or recognition index for time of exploration (0.65 ± 0.07 vs. 0.64 ± 0.08, respectively; $P = 0.94$). On day 2, the CNI-1493–treated animals tended to investigate more novel objects (recognition index for number of exploration: 0.68 ± 0.06 vs. 0.50 ± 0.07, respectively; $P = 0.061$) and spent significantly more time with the novel objects (recognition index for time of exploration: 0.74 ± 0.05 vs. 0.52 ± 0.08, respectively; $P = 0.024$) than placebo-treated animals (Fig. 6). Collectively, these data indicate that CNI-1493 treatment is therapeutic in an animal model of AD. CNI-1493 treatment not only decreases

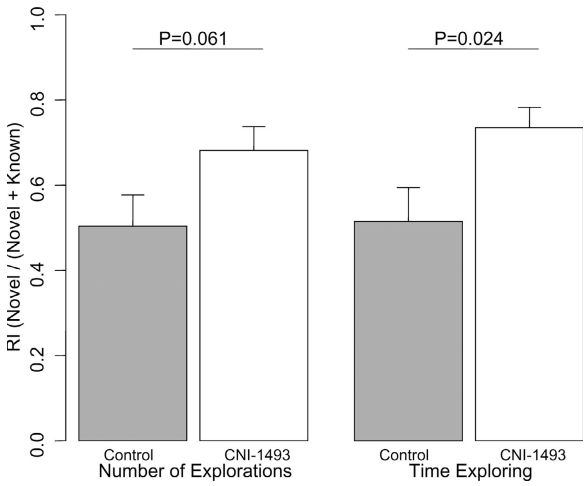

Figure 6. Novel object task. The recognition indices (RI) for number and length of time spent exploring the novel object is given for control-treated (shaded bars) and CNI-1493–treated (open bars) animals. The RI represents the proportion of object exploration that was spent exploring the novel object. Statistics, two sample Student's *t* test; RiN, P = 0.061; RiT, P = 0.024; Control, *n* = 12; CNI-1493, *n* = 13. Error bars represent the SEM.

amyloid plaque formation but also preserves the cognitive ability of the mice to investigate their surroundings more fully.

The major finding of this study is the efficacy of the potent macrophage deactivator CNI-1493 in a murine Aβ plaque deposition model. CNI-1493 not only suppresses the development of Aβ plaques but also improves cognitive function after 2 mo of treatment in TgCRND8 mice, which overexpress the human APP. As anticipated, CNI-1493 treatment is accompanied by microglial deactivation. Moreover, our in vitro analysis of CNI-1493 treatment on APP processing in an APP-overexpressing cell line suggests a profound dose-dependent decrease of total Aβ secretion. This effect appears to be completely separate from both the production of APP and altered β- or γ-secretase activities. Thus, CNI-1493 may have a dual beneficial role in mice by inhibiting microglial activation and by promoting Aβ clearance. Although further work will be needed to determine whether these two mechanisms of action are causally linked, the results presented herein identify the antiinflammatory agent CNI-1493 as a very promising candidate for the treatment and prevention of AD in clinical trials.

MATERIALS AND METHODS

CNI-1493. CNI-1493 was synthesized as previously described (23).

ELISA assay. Aβ 42 oligomers (0.3 mg Aβ/ml H_2O) were prepared with and without CNI-1493, as described previously (10). Samples were diluted to 50 ng/100 μl in coating buffer (0.1 M sodium bicarbonate, pH 9.6), and 100 μl of the samples were added to wells of 96-well microplates, incubated for 1 h at 37°C, washed three times with TBS containing 0.01% Tween 20 (TBS-T), and then blocked for 2 h at 37°C with 10% BSA/TBS-T. The plates were washed three times with PBS-T and 100 μl of anti-Aβ oligomer antiserum (1:2,000 dilution in 5% nonfat milk/TBS-T) was added and incubated for 1 h at 37°C. The plates were washed three times with PBS-T and 100 μl horseradish peroxidase–conjugated anti–rabbit IgG (diluted 1:10,000 in 5% nonfat milk/TBS-T; Promega) was added and incubated for 1 h at 37°C. The plates were washed three times with PBS-T and developed using 3,3′,5,5′-tetramethylbenzidine (KP). The reaction was stopped with 100 μl 1 M HCl and the plates were read at 450 nm.

Animals. All animal procedures were approved by the office of the district president and the Institutional Animal Care and Use Committee for the University of Munster. We used the TgCRND8 mouse line (courtesy of D. Westaway, University of Toronto, Toronto, Canada). TgCRND8 mice encode a double-mutant form of APP 695 (KM670/671NL+V717F) under the control of the PrP gene promoter (24). Thioflavine S–positive Aβ amyloid deposits are present at 3 mo, with dense-cored plaques and neuritic pathology evident from 5 mo of age. TgCRND8 mice exhibit 3,200–4,600 pmol of Aβ per gram of brain at age 6 mo, with an excess of Aβ 42 over Aβ 40.

Drug treatment of TgCRND8 mice. 10 APP transgenic TgCRND8 mice at 4 mo of age received an i.p. injection of either 200 μl placebo or 200 μl containing 200 μg (8 mg/kg) CNI-1493 twice a week for 8 wk. One animal of the CNI-1493 group died before completion of the 16 injections and was excluded from further analysis. Mice were housed in groups of 3–4 animals in standard (37(l) × 21 (w) × 15 (h) cm) cages accompanied by wild-type littermates. At the end of the experimental period, animals were killed and the brain hemispheres were separated along the midline. One hemisphere was fixed in 4% buffered formaldehyde for 24 h, followed by dehydration and paraffin embedding. The other hemisphere was immediately snap-frozen in liquid nitrogen and kept at −80°C until use.

Electron microscopy studies. Aβ oligomers were prepared at a concentration of 40–55 μM as previously described (10). Aβ oligomers were incubated with CNI-1493 at 1:10 ratios for 20 min with mixing. 2 μl of this solution were adsorbed onto 200 mesh Nickle carbon– and formvar-coated grids, air dried, and washed for 30 s in distilled water. The samples were negatively stained with 2% uranyl acetate (Ted Pella, Inc.) for 2 min and viewed with a 10CR microscope (80 kV; Carl Zeiss, Inc.).

Toxicity assays. MTT toxicity assay was performed as previously described (10) using SH-SY5Y human neuroblastoma cells. Cells were treated with Aβ oligomers at a final concentration of 2.5 μM, and samples with CNI-1493 were incubated for 15 min before treatment. Each data point was determined in hexaplicate.

Immunohistochemistry. Three pairs of 2-μm sagittal brain sections of each transgenic animal were stained for Aβ immunoreactivity. The pairs (10 μm distance) were situated 100, 200, and 300 μm lateral from the midsagittal fissure. All slices were pretreated with formic acid and automatically stained in a TechMate Instrument (Dako) with 6F/3D anti-Aβ monoclonal antibody to residues 8–17 (Dako; 1:100). For further steps, the StreptABC complex/horseradish peroxidase–conjugated "Duet" anti–mouse/–rabbit antibody kit (Dako) was used and developed with 3, 3′-diaminobenzidine as chromogen. Counterstaining was performed with hematoxylin. All slides were stained in two consecutive procedures, making sure that brains of both experimental groups were equally distributed in both procedures.

Image analysis. To quantify Aβ plaque burden, cortices and hippocampus of all stained sections were digitalized by a ColorView II, 3, 3 Mega Pixel charge-coupled device camera under constant light and filter settings. Color images were converted to grayscale to obtain the best contrast between positive immunoreactivity and background. A constant threshold was chosen for all images to detect immunoreactive staining. Morphometric measurements were performed using SIS analysis Auto Software 3.2 (Soft Imaging System). The total number and size of plaques was related to the total area analyzed.

Biochemical analysis. Half of the brain was weighed and homogenized in an appropriate volume of T-PER (Perbio) in accordance with the guidelines of the manufacturer. Protein concentrations of the lysates were measured by BCA kit (Perbio). Samples (15–60 μg protein) were loaded onto precast NuPAGE Novex 4–12% Bis-Tris gel using the Novex electrophoresis system (Invitrogen). Subsequently, the proteins were transferred onto nitrocellulose membranes (Invitrogen) using the XCell II blot (Invitrogen). The immobilized proteins were visualized using MemCode reversible protein staining kit (Perbio). The membranes were blocked overnight at 4°C in Roti-Block (Roth). For the detection of membrane-bound Aβ, we added 6E10 monoclonal antibodies (Biodesign) as primary detection antibodies at a dilution of 1:1,000 for 1 h at ambient temperature on a roller shaker. The membranes were washed 4 times with PBS containing 0.05% Tween 20, and incubated for 1 h with horseradish peroxidase–conjugated secondary goat anti–mouse IgG (Perbio) at a 1:250,000 dilution. The blots were washed 4 times for 10 min, incubated for 5 min in SuperSignal West Dura Extended Duration Substrate working solution (Perbio) and exposed to an autoradiographic film (T-Mat Plus DG Film; Kodak). Alternatively, membranes were hybridized with rat anti–mouse F4/80 antibodies (Serotec). Equal protein loading of all membranes was assessed by reprobing with monoclonal antibodies against GAPDH (Acris).

APP processing analysis in N2a cells. APP_{695}-transfected N2a cells (25) were grown in 1:1 DME/Opti-MEM supplemented with 5% FBS, penicillin, and streptomycin, and 0.2 mg/ml G418. Cells were treated at confluency for 24 h with the indicated concentrations of CNI-1493. Medium was then changed and treatments were continued for another 2 h to allow Aβ secretion. 20 μl of conditioned medium were electrophoresed on 16.5% Tris-Tricine gels and transferred onto 0.2-μm nitrocellulose membranes. Membranes were then microwaved for 5 min in PBS, blocked in 5% fat-free milk in TBS, and incubated with 6E10 (Signet; 1:1,000 SuperBlock; Thermo Fisher Scientific) overnight at 4°C. Cells were washed with PBS and solubilized in ice-cold Hepes buffer (25 mM Hepes, pH 7.4, 150 mM NaCl, and 1X Complete protease inhibitor cocktail [Roche]) containing 1% SDS. 10 μg of extracts were analyzed by WB with 6E10, R1 (anti-APP C-terminal domain), and LN27 (anti-APP_{1-200}; Invitrogen).

Cognition tests. Of the 33 initial male hemizygous TgCRND8 mice that were chosen for characterizing learning and memory performance 28 survived until completion of the tests. Live expectancy of TgCRND8 mice is known to be slightly reduced in hemizygous animals compared with wild-types (24). Of the five animals that died during the course of the investigation, three were injected with placebo and two with CNI-1493. None of the CNI-1493–treated animals died within 48 h after an injection. Mice were housed in standard (37 [l] × 21 [w] × 15 [h] cm) cages accompanied by wild-type littermates for up to five animals per cage. Once a week, mice were transferred to clean cages and, if necessary, fur cuts that allowed individual discrimination of the mice were renewed. All animals lived in a light–dark cycle of 12:12 h, with lights on between 0700 and 1900 h. The cages contained a thin layer of wood shavings (Allspan, Höveler GmbH & Co.) and paper towels as nesting material. Food (Altromin 1324; Altromin GmbH) and tap water was available ad libitum.

The room temperature was maintained at 22 ± 2°C, relative humidity was maintained at 45 ± 10%. Mice were injected twice a week (Tuesday and Friday) between day 90 ± 3 and 142 ± 3, with either 200 μl placebo or 200 μl CNI-1493 (10/190 μl). Assignment to treatment groups was done randomly, and the experimenter was not aware of the treatment of individual mice. Experimental scheduling was done using FMDB software (26).

All procedures and protocols met the guidelines for animal care and animal experiments in accordance with national and European (86/609/EEC) legislation.

Barnes maze. Spatial memory was analyzed using a circular platform of 1 m diam with 12 holes equally distributed close to the edge. Mice were placed on the center of the platform and time taken, path length covered, and errors made (exploring wrong holes) were recorded by a tracking system until the mice escaped from the platform by entering the target hole that led back to their homecage, which was placed below the platform. The test was repeated twice a day on 5 consecutive days, allowing time to derive learning curves for the aforementioned measures. Details are available in a previous study (27).

Novel object task. Object recognition memory was analyzed with the novel object task (28). The test is based upon the tendency of mice to investigate a novel object rather than a familiar one. To facilitate exploration mice were handled 1 wk before the test and additionally habituated to the test arena (30 × 30 cm plywood box, with walls 40 cm high) for 5 min per day over a period of 3 d before testing. The task was independently conducted two times on two consecutive days with mice being 145 ± 3 d of age. In a first trial (training phase) on each day the mice were allowed to explore two similar objects for 5 min. After 1 h, the mouse again was placed into the open field now containing one object similar to both objects presented in the first trial and one novel object (choice phase). A total of five different objects made of biologically neutral material, such as plastic or metal, were used. The objects were not known to have any ethological significance for the mice, and they were never associated with a reinforcer, as recommended by Ennaceur (29). To avoid object or place preferences, place and novelty status was changed for each object in regular intervals. Fecal boli were removed, and the walls and the floor of the open field arena were cleaned with ethanol (70%) after each tested animal. Number and length of time spent exploring the objects were recorded using the "Novel Object Task" software and a handheld computer (http://www.phenotyping.com/not.html). Mice that did not explore any of the objects in either the training phase or the choice phase could not be analyzed regarding recognition processes, and thus were excluded from the analysis of learning behavior on this test day (day 1: 2 CNI-1493-, 2 placebo-treated mice; day 2: 1 CNI-1493-, 2 placebo-treated mice). To compare the performance of both treatment groups, the recognition indices were calculated as follows: RiN, number of exploration of novel object/total number of object explorations; RiT, time spent exploring novel object/total time spent exploring objects. Indices above chance level (0.5) reflect a preference for the novel object over the known object, and thus indicate object recognition memory.

Statistics. Data were analyzed using either Student's *t* tests or, when datasets showed a non-Gaussian distribution, nonparametric Mann-Whitney *U* tests were applied (30). A significance-level (α) of 0.05 was selected. All tests were performed two sided.

Online supplemental material. Fig. S1 shows that CNI-1493 does not prevent staurosporine-induced cytotoxicity. Fig. S2 shows that CNI-1493 inhibits soluble Aβ formation in transgenic APP TgCRND8 mice. The online version of this article is available at http://www.jem.org/cgi/content/full/jem.20060467/DC1.

The authors thank Drs. Kevin Tracey and Thomas Coleman for their careful and critical reading of the manuscript. We also thank Meredith Akerman for her help with the statistical analysis of the cognition data.

YAA thanks the Alzheimer Drug Discovery Foundation for funding portions of this work.

YAA holds stock options in Cytokine PharmaSciences, Inc. which owns patent rights in CNI-1493 and certain uses thereof. The authors have no other conflicting financial interests.

Submitted: 28 February 2006
Accepted: 8 May 2008

REFERENCES

1. Selkoe, D.J. 2001. Alzheimer's disease: genes, proteins, and therapy. *Physiol. Rev.* 81:741–766.
2. Hardy, J., and M. Mullan. 1992. Alzheimer's disease. In search of the soluble. *Nature.* 359:268–269.

3. Golde, T.E., C.B. Eckman, and S.G. Younkin. 2000. Biochemical detection of Abeta isoforms: implications for pathogenesis, diagnosis, and treatment of Alzheimer's disease. *Biochim. Biophys. Acta.* 1502:172–187.
4. Younkin, S.G. 1998. The role of A beta 42 in Alzheimer's disease. *J. Physiol. (Paris).* 92:289–292.
5. Walsh, D.M., I. Klyubin, J.V. Fadeeva, W.K. Cullen, R. Anwyl, M.S. Wolfe, M.J. Rowan, and D.J. Selkoe. 2002. Naturally secreted oligomers of amyloid beta protein potently inhibit hippocampal long-term potentiation in vivo. *Nature.* 416:535–539.
6. Selkoe, D.J. 2002. Alzheimer's disease is a synaptic failure. *Science.* 298:789–791.
7. Pitschke, M., R. Prior, M. Haupt, and D. Riesner. 1998. Detection of single amyloid beta-protein aggregates in the cerebrospinal fluid of Alzheimer's patients by fluorescence correlation spectroscopy. *Nat. Med.* 4:832–834.
8. Lue, L.F., Y.M. Kuo, A.E. Roher, L. Brachova, Y. Shen, L. Sue, T. Beach, J.H. Kurth, R.E. Rydel, and J. Rogers. 1999. Soluble amyloid beta peptide concentration as a predictor of synaptic change in Alzheimer's disease. *Am. J. Pathol.* 155:853–862.
9. McLean, C.A., R.A. Cherny, F.W. Fraser, S.J. Fuller, M.J. Smith, K. Beyreuther, A.I. Bush, and C.L. Masters. 1999. Soluble pool of Abeta amyloid as a determinant of severity of neurodegeneration in Alzheimer's disease. *Ann. Neurol.* 46:860–866.
10. Kayed, R., E. Head, J.L. Thompson, T.M. McIntire, S.C. Milton, C.W. Cotman, and C.G. Glabe. 2003. Common structure of soluble amyloid oligomers implies common mechanism of pathogenesis. *Science.* 300:486–489.
11. Akiyama, H., S. Barger, S. Barnum, B. Bradt, J. Bauer, G.M. Cole, N.R. Cooper, P. Eikelenboom, M. Emmerling, B.L. Fiebich, et al. 2000. Inflammation and Alzheimer's disease. *Neurobiol. Aging.* 21:383–421.
12. McGeer, P.L., M. Schulzer, and E.G. McGeer. 1996. Arthritis and anti-inflammatory agents as possible protective factors for Alzheimer's disease: a review of 17 epidemiologic studies. *Neurology.* 47:425–432.
13. Bianchi, M., O. Bloom, T. Raabe, P.S. Cohen, J. Chesney, B. Sherry, H. Schmidtmayerova, T. Calandra, X. Zhang, M. Bukrinsky, et al. 1996. Suppression of proinflammatory cytokines in monocytes by a tetravalent guanylhydrazone. *J. Exp. Med.* 183:927–936.
14. Martiney, J.A., A.J. Rajan, P.C. Charles, A. Cerami, P.C. Ulrich, S. Macphail, K.J. Tracey, and C.F. Brosnan. 1998. Prevention and treatment of experimental autoimmune encephalomyelitis by CNI-1493, a macrophage-deactivating agent. *J. Immunol.* 160:5588–5595.
15. Meistrell, M.E. III, G.I. Botchkina, H. Wang, E. Di Santo, K.M. Cockroft, O. Bloom, J.M. Vishnubhakat, P. Ghezzi, and K.J. Tracey. 1997. Tumor necrosis factor is a brain damaging cytokine in cerebral ischemia. *Shock.* 8:341–348.
16. Kerlund, K., H. Erlandsson Harris, K.J. Tracey, H. Wang, T. Fehniger, L. Klareskog, J. Andersson, and U. Andersson. 1999. Anti-inflammatory effects of a new tumour necrosis factor-alpha (TNF-alpha) inhibitor (CNI-1493) in collagen-induced arthritis (CIA) in rats. *Clin. Exp. Immunol.* 115:32–41.
17. Yan, Q., J. Zhang, H. Liu, S. Babu-Khan, R. Vassar, A.L. Biere, M. Citron, and G. Landreth. 2003. Anti-inflammatory drug therapy alters beta-amyloid processing and deposition in an animal model of Alzheimer's disease. *J. Neurosci.* 23:7504–7509.
18. Lim, G.P., F. Yang, T. Chu, P. Chen, W. Beech, B. Teter, T. Tran, O. Ubeda, K.H. Ashe, S.A. Frautschy, and G.M. Cole. 2000. Ibuprofen suppresses plaque pathology and inflammation in a mouse model for Alzheimer's disease. *J. Neurosci.* 20:5709–5714.
19. Ezekowitz, R.A., J. Austyn, P.D. Stahl, and S. Gordon. 1981. Surface properties of bacillus Calmette-Guerin-activated mouse macrophages. Reduced expression of mannose-specific endocytosis, Fc receptors, and antigen F4/80 accompanies induction of Ia. *J. Exp. Med.* 154:60–76.
20. Weggen, S., J.L. Eriksen, P. Das, S.A. Sagi, R. Wang, C.U. Pietrzik, K.A. Findlay, T.E. Smith, M.P. Murphy, T. Bulter, et al. 2001. A subset of NSAIDs lower amyloidogenic Abeta42 independently of cyclooxygenase activity. *Nature.* 414:212–216.
21. Barnes, C.A. 1979. Memory deficits associated with senescence: a neurophysiological and behavioral study in the rat. *J. Comp. Physiol. Psychol.* 93:74–104.
22. Powell, S.B., M.A. Geyer, D. Gallagher, and M.P. Paulus. 2004. The balance between approach and avoidance behaviors in a novel object exploration paradigm in mice. *Behav. Brain Res.* 152:341–349.
23. Bianchi, M., P. Ulrich, O. Bloom, M. Meistrell III, G.A. Zimmerman, H. Schmidtmayerova, M. Bukrinsky, T. Donnelley, R. Bucala, B. Sherry, et al. 1995. An inhibitor of macrophage arginine transport and nitric oxide production (CNI-1493) prevents acute inflammation and endotoxin lethality. *Mol. Med.* 1:254–266.
24. Chishti, M.A., D.S. Yang, C. Janus, A.L. Phinney, P. Horne, J. Pearson, R. Strome, N. Zuker, J. Loukides, J. French, et al. 2001. Early-onset amyloid deposition and cognitive deficits in transgenic mice expressing a double mutant form of amyloid precursor protein 695. *J. Biol. Chem.* 276:21562–21570.
25. Marambaud, P., H. Zhao, and P. Davies. 2005. Resveratrol promotes clearance of Alzheimer's disease amyloid-beta peptides. *J. Biol. Chem.* 280:37377–37382.
26. Lewejohann, L. 2007. Fill my datebook: a software tool to generate and handle lists of events. *Behav. Res. Methods.* 40:391–393.
27. Ambree, O., H. Ritcher, N. Sachser, L. Lewejohann, E. Dere, M. de Souza Silva, A. Herring, K. Keyvani, W. Paulus, and W. Schaebitz. 2008. Levodopa ameliorates learning and memory deficits in a murine model of Alzheimer's disease. *Neurobiol. Aging.* In press.
28. Ennaceur, A., and J. Delacour. 1988. A new one-trial test for neurobiological studies of memory in rats. 1: Behavioral data. *Behav. Brain Res.* 31:47–59.
29. Ennaceur, A., S. Michalikova, A. Bradford, and S. Ahmed. 2005. Detailed analysis of the behavior of Lister and Wistar rats in anxiety, object recognition and object location tasks. *Behav. Brain Res.* 159:247–266.
30. Siegel, S. 1956. Non-parametric statistics for the behavioral sciences. McGraw Hill, New York.